

# Generalized theoretical analysis method for free-edge delaminations in composite laminates

IN-GWON KIM, CHANG-DUK KONG

Department of Aerospace Eng., Chosun University, 375 Seosuk-dong, Gwangju, Korea  
E-mail: inkkim@mail.chosun.ac.kr

N. UDA

Department of Aerospace Eng., Kyushu University, Fukuoka, Japan

A simplified method for determining the individual mode components of the strain energy release rate of free-edge delaminations in composite laminates is proposed. Interlaminar stresses are evaluated as an interface moment and interface shear forces obtained from equilibrium equations of stress resultants at the interface between the adjacent layers. The deformation of edge-delaminated laminate is calculated by using a generalized quasi-three dimensional classical laminated plate theory developed by the authors. The analysis provides closed-form expressions for the Mode-I, Mode-II and Mode-III component of the strain energy release rate by combining the deformation of the edge-delaminated laminate with the interface moment and the interface shear forces. The presented method is compared with existing method suggested by Li for the asymmetry laminate. Comparison of the results with a finite element analysis using the virtual crack closure technique shows good agreement. © 2002 Kluwer Academic Publishers

## 1. Introduction

Delaminations along the free edges of composite laminates under uniform axial strain as shown in Fig. 1 have been observed during testing and in service. The free-edge delaminations induce redistribution of the stresses in the piles of laminate, and, therefore, usually result in a reduction of stiffness and strength of the laminate. A number of experimental and analytical investigations have been directed toward well understanding of free-edge delamination mechanisms. Pipes and Pagano [1] proposed a quasi-three dimensional (Q3D) analysis for a symmetric laminate under uniform axial extension. They showed the interlaminar stress distribution by the finite difference technique based on the Q3D analysis, and pointed out that the free-edge delaminations are caused by the interlaminar stresses which arise in the vicinity of the free edge. Rybicki, Schmueser and Fox [2] and Wang and Crossman [3] evaluated the strain energy release rate (SERR) by using a finite element method (FEM) with the virtual crack closure technique. These previous works have shown that the delamination onset and growth can be characterized quantitatively by the SERR.

In order to estimate the SEER, O'Brien [4] developed a simple expression based on the classical laminated plate theory (CLT) and the rule of mixtures. Aoki and Kondo [5] proposed a method based on the  $J$ -integral law in combination with the CLT for calculating the Mode-I component of SERR. Armanions and Rehfield [6] used a sublaminar analysis with a shear deformable plate theory to determine the individual mode components of SERR. Schapery and Davidson [7] proposed

a crack tip element approach, which is a method combined a sublaminar analysis based on the CLT with FEM, for determining mode ratio of SERR. Kunoo *et al.* [8] presented a generalized quasi-three dimensional classical laminated plate theory (GQ3D-CLT) to obtain the SERR.

The objective of the presented work is to develop a simplified method for determining the individual mode components of SERR. The method is based on the GQ3D-CLT. The analysis provides closed-form expressions for the Mode-I, Mode-II and Mode-III component of SERR.

## 2. Formulation

### 2.1. Evaluation of interlaminar stresses

Classical laminated plate theory (CLT) assumes that the states of stress within each lamina of a multidirectional laminate are planar. This assumption is accurate for inner region away from laminate geometric discontinuities, such as a free edge. In the vicinity of the free edge a boundary exists where the state of stress is three-dimensional. The boundary width is approximately equal to the overall laminate thickness [1]. The stresses, which arise at the interface between adjacent layers in the boundary, are called interlaminar stresses. A lot of studies have been made to analyze the distribution of the interlaminar stresses. In this paper, we evaluate indirectly the interlaminar stresses as stress resultants instead of calculating the interlaminar stress distribution. CLT gives the inplane stresses,  $\sigma_y$  and  $\tau_{xy}$ , shown in Fig. 2. These in-plane stresses vanish at the

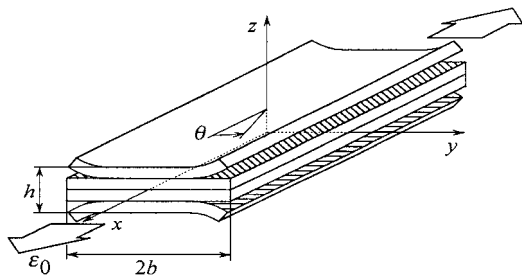


Figure 1 A laminate with free-edge delaminations and coordinate system.

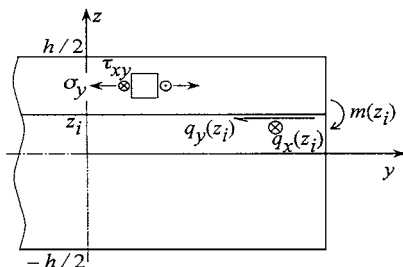


Figure 2 Definition of interface moment and interface shear forces.

free edge of the laminate. By using equilibrium equation of stress resultants at the interface  $z = z_i$  in the boundary, we define an interface moment,  $m(z_i)$ , [9] and interface shear forces,  $q_y(z_i)$  and  $q_x(z_i)$ , as follows.

The interface moment,  $m(z_i)$ , is reacted by the interlaminar normal stress component,  $\sigma_z$ . The distribution of the interlaminar normal stress must, therefore, result in zero vertical force vector while producing a moment equal in magnitude to that given by the first equation of Equation 1. When the interface moment is positive, the interlaminar normal stress  $\sigma_z$  is tensile in the boundary near the free edge. It means that a peeling stress occurs at the interface in the free-edge boundary and delamination crack with the opening mode (Mode I) may be generated.

$$\begin{aligned} m(z_i) &= \int_{z_i}^{h/2} \sigma_y(z)(z - z_i) dz \\ q_y(z_i) &= - \int_{z_i}^{h/2} \sigma_y(z) dz \\ q_x(z_i) &= - \int_{z_i}^{h/2} \tau_{xy}(z) dz \end{aligned} \quad (1)$$

The interface shear forces,  $q_y(z_i)$  and  $q_x(z_i)$ , are reacted by the interlaminar shear stress components,  $\tau_{yz}$  and  $\tau_{xz}$ , respectively. When the interface shear force is not zero, the interlaminar shear stress occurs at the interface in the free-edge boundary. In the case of  $q_y(z_i) \neq 0$ , delamination crack with the in-plane shear mode (Mode II) may be generated. In the case of  $q_x(z_i) \neq 0$ , delamination crack with the anti-plane shear mode (Mode III) may be generated.

## 2.2. Generalized quasi-three dimensional classical laminated plate theory

Pipes and Pagano [1] proposed the following quasi-three dimensional (Q3D) displacement field equations

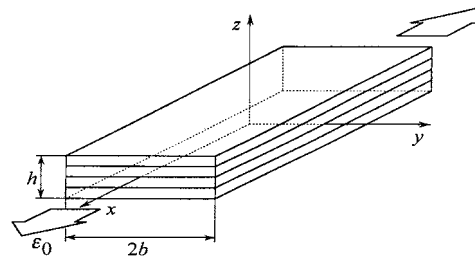


Figure 3 Quasi-three dimensional problems.

for symmetric laminate under uniform axial strain as shown in Fig. 3.

$$\begin{aligned} u(x, y, z) &= U(y, z) + \epsilon_0 x \\ v(x, y, z) &= V(y, z) \\ w(x, y, z) &= W(y, z) \end{aligned} \quad (2)$$

where  $\epsilon_0$  is uniform axial strain. These Q3D displacement field equations, however, are not applicable to asymmetric laminates. Hence we derived the following displacement field equations for asymmetric laminates [8].

$$\begin{aligned} u(x, y, z) &= U(y, z) + (C_1 + C_4 y + C_2 z)x \\ v(x, y, z) &= V(y, z) - \left( \frac{1}{2} C_4 x - C_3 z \right) x \\ w(x, y, z) &= W(y, z) - \left( \frac{1}{2} C_2 x + C_3 y \right) x \end{aligned} \quad (3)$$

We called Equation 3 as generalized quasi-three dimensional (GQ3D) displacement field equations. While the parameter  $C_1$  is equivalent to  $\epsilon_0$ , which describes uniform axial strain of a laminate, the GQ3D equations include additional parameters  $C_2$ ,  $C_3$  and  $C_4$ .  $C_2$  and  $C_4$  represent bending deformations of a laminate, and  $C_3$  represents twisting deformation of a laminate.

We derive a generalized quasi-three dimensional classical laminated plate theory (GQ3D-CLT) by applying the GQ3D displacement field equations (3) to CLT. CLT gives the in-plane strain components of a laminate as follows.

$$\begin{aligned} \epsilon_x &= \epsilon_x^0 + z\kappa_x, & \epsilon_y &= \epsilon_y^0 + z\kappa_y, & \gamma_{xy} &= \gamma_{xy}^0 + z\kappa_{xy} \end{aligned} \quad (4)$$

where

$$\begin{aligned} \epsilon_x^0 &= \frac{\partial u^0}{\partial x}, & \epsilon_y^0 &= \frac{\partial v^0}{\partial y}, & \gamma_{xy}^0 &= \frac{\partial u^0}{\partial y} + \frac{\partial v^0}{\partial x}, \\ \kappa_x &= -\frac{\partial^2 w^0}{\partial x^2}, & \kappa_y &= -\frac{\partial^2 w^0}{\partial y^2}, & \kappa_{xy} &= -2\frac{\partial^2 w^0}{\partial x \partial y}. \end{aligned} \quad (5)$$

$u^0$ ,  $v^0$  and  $w^0$  are displacements at the mid-plane of the laminate. On the other hand, we get the following  $x$ -direction strain by using the GQ3D displacement

field equations (3).

$$\varepsilon_x = \frac{\partial u}{\partial x} = C_1 + C_4 y + C_2 z \quad (6)$$

Comparing Equation 6 with Equation 4, we obtain the following relations.

$$C_1 + C_4 y = \varepsilon_x^0, \quad C_2 = \kappa_x \quad (7)$$

We consider the laminate under uniform axial strain  $\varepsilon_0$ . Therefore,

$$C_1 = \varepsilon_0 \quad (8)$$

Introducing the curvature  $\omega_x$  with respect to the in-plane bending moment, we get the following equation.

$$C_4 = \omega_x \quad (9)$$

Substituting the GQ3D displacement field equations (3) to the last equation of Equation 5, we obtain

$$C_3 = \kappa_{xy} \quad (10)$$

We can find that the GQ3D displacement field equations (3) are applicable to analyzing a laminate under the bending deformations,  $\kappa_x$  and  $\omega_x$ , and the twisting deformation  $\kappa_{xy}$  in addition to axial extension  $\varepsilon_0$ , as shown in Fig. 4.

CLT defines the resultant forces and moments as follows,

$$\begin{Bmatrix} N_x \\ N_y \\ N_{xy} \end{Bmatrix} = \int_{z_1}^{z_2} \begin{Bmatrix} \sigma_x \\ \sigma_y \\ \tau_{xy} \end{Bmatrix} dz, \quad \begin{Bmatrix} M_x \\ M_y \\ M_{xy} \end{Bmatrix} = \int_{z_1}^{z_2} \begin{Bmatrix} \sigma_x \\ \sigma_y \\ \tau_{xy} \end{Bmatrix} z dz \quad (11)$$

where  $z_1$ , and  $z_2$  are coordinates of the  $yz$  section. GQ3D-CLT, however, treats the resultant forces and moments shown in Fig. 5. CLT does not include a resultant moment  $T_x$  corresponding to the curvature  $\omega_x$ . In addition, CLT defines Equation 11 as forces and moments per unit width of the  $yz$  section because of the infinite plate assumption of CLT. Hence we employ the

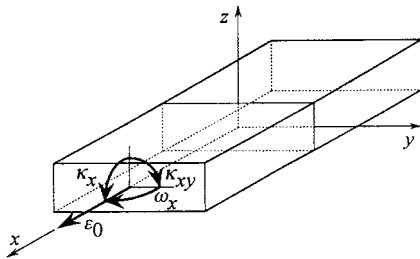


Figure 4 Generalized quasi-three dimensional problems.

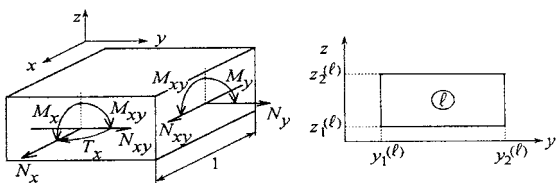


Figure 5 Resultant forces and moments acting on a laminate with finite width.

following definitions for the resultant forces and moments acting on the laminate with finite width ( $y_2 - y_1$ ) as shown in Fig. 5.

$$\begin{Bmatrix} N_x \\ N_y \\ N_{xy} \end{Bmatrix} = \int_{z_1}^{z_2} \int_{y_1}^{y_2} \begin{Bmatrix} \sigma_x \\ \sigma_y \\ \tau_{xy} \end{Bmatrix} dy dz, \quad \begin{Bmatrix} M_x \\ M_y \\ M_{xy} \end{Bmatrix} = \int_{z_1}^{z_2} \int_{y_1}^{y_2} \begin{Bmatrix} \sigma_x \\ \sigma_y \\ \tau_{xy} \end{Bmatrix} z dy dz \quad (12)$$

$$T_x = \int_{z_1}^{z_2} \int_{y_1}^{y_2} \sigma_x y dy dz$$

The stress-strain relations for the  $k$ -th layer of a multilayered laminate can be written as

$$\begin{Bmatrix} \sigma_x \\ \sigma_y \\ \sigma_{xy} \end{Bmatrix}_k = \begin{bmatrix} \bar{Q}_{11} & \bar{Q}_{12} & \bar{Q}_{16} \\ \bar{Q}_{12} & \bar{Q}_{22} & \bar{Q}_{26} \\ \bar{Q}_{16} & \bar{Q}_{26} & \bar{Q}_{66} \end{bmatrix}_k \begin{Bmatrix} \varepsilon_x \\ \varepsilon_y \\ \gamma_{xy} \end{Bmatrix} \quad (13)$$

$$= \begin{bmatrix} \bar{Q}_{11} & \bar{Q}_{12} & \bar{Q}_{16} \\ \bar{Q}_{12} & \bar{Q}_{22} & \bar{Q}_{26} \\ \bar{Q}_{16} & \bar{Q}_{26} & \bar{Q}_{66} \end{bmatrix}_k \left( \begin{Bmatrix} \varepsilon_0 \\ \varepsilon_y^0 \\ \gamma_{xy}^0 \end{Bmatrix} + z \begin{Bmatrix} \kappa_x \\ \kappa_y \\ \kappa_{xy} \end{Bmatrix} + y \begin{Bmatrix} \omega_x \\ 0 \\ 0 \end{Bmatrix} \right)$$

Substituting Equation 13 to Equation 12, we can get the following constitutive equations for the GQ3D-CLT.

$$\begin{Bmatrix} N_x \\ N_y \\ N_{xy} \\ M_x \\ M_y \\ M_{xy} \\ T_x \end{Bmatrix} = \begin{bmatrix} A_{11} & A_{12} & A_{16} & B_{11} & B_{12} & B_{16} & C_{11} \\ A_{12} & A_{22} & A_{26} & B_{12} & B_{22} & B_{26} & C_{12} \\ A_{16} & A_{26} & A_{66} & B_{16} & B_{26} & B_{66} & C_{16} \\ B_{11} & B_{12} & B_{16} & D_{11} & D_{12} & D_{16} & E_{11} \\ B_{12} & B_{22} & B_{26} & D_{12} & D_{22} & D_{26} & E_{12} \\ B_{16} & B_{26} & B_{66} & D_{16} & D_{26} & D_{66} & E_{16} \\ C_{11} & C_{12} & C_{16} & E_{11} & E_{12} & E_{16} & F_{11} \end{bmatrix} \begin{Bmatrix} \varepsilon_0 \\ \varepsilon_y^0 \\ \gamma_{xy}^0 \\ \kappa_x \\ \kappa_y \\ \kappa_{xy} \\ \omega_x \end{Bmatrix} \quad (14)$$

where

$$[A_{ij}, B_{ij}, D_{ij}] = (y_2 - y_1) \sum_{k=1}^N (\bar{Q}_{ij})_k \left[ (z_k - z_{k-1}), \frac{1}{2}(z_k^2 - z_{k-1}^2), \frac{1}{3}(z_k^3 - z_{k-1}^3) \right] \quad (15)$$

$$[C_{ij}, E_{ij}] = \frac{1}{2}(y_2^2 - y_1^2) \sum_{k=1}^N (\bar{Q}_{ij})_k \left[ (z_k - z_{k-1}), \frac{1}{2}(z_k^2 - z_{k-1}^2) \right]$$

$$F_{11} = \frac{1}{3}(y_2^3 - y_1^3) \sum_{k=1}^N (\bar{Q}_{ij})_k (z_k - z_{k-1})$$

### 2.3. Analysis of a laminate with a free-edge delamination by GQ3D-CLT

We consider a laminate with a free-edge delamination under uniform axial strain. The laminate is divided into three sublaminates as shown in Fig. 6.

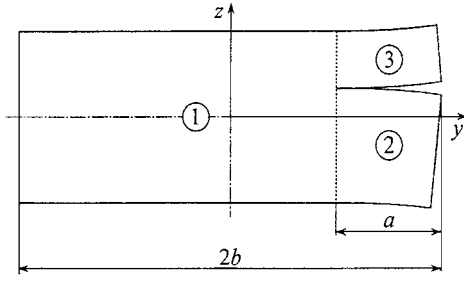


Figure 6 Description of sublaminates.

The delamination length is denoted by  $a$ . Sublaminates 2 and 3 represent the groups of plies below and above the interface along which delamination occurs, respectively. Because the forces,  $N_y$ , and  $N_{xy}$ , and the moment,  $M_y$ , are not reacted on the laminate under uniform axial strain, the following conditions should be satisfied for each sublaminates.

$$N_y^{(\lambda)} = N_{xy}^{(\lambda)} = M_y^{(\lambda)} = 0 \quad (16)$$

Where superscript  $(\lambda)$  denotes the  $\lambda$ -th sublaminates. Hence we get the following reduced constitutive equations for the  $\lambda$ -th sublaminates.

$$\tilde{N}^{(\lambda)} = \tilde{H}^{(\lambda)} \tilde{C}^{(\lambda)} \quad (17)$$

where

$$\tilde{N}^{(\lambda)} = \begin{Bmatrix} N_x \\ M_x \\ M_{xy} \\ T_x \end{Bmatrix}^{(\lambda)}, \quad \tilde{C}^{(\lambda)} = \begin{Bmatrix} \varepsilon_0 \\ \kappa_x \\ \kappa_{xy} \\ \omega_x \end{Bmatrix}^{(\lambda)} \quad (18)$$

$$\tilde{H}^{(\lambda)} = \begin{bmatrix} A'_{11} & B'_{11} & B'_{16} & C'_{11} \\ B'_{11} & D'_{11} & D'_{16} & E'_{11} \\ B'_{16} & D'_{16} & D'_{66} & E'_{16} \\ C'_{11} & E'_{11} & E'_{16} & F'_{11} \end{bmatrix}^{(\lambda)}$$

The vectors  $\tilde{C}^{(1)}$ ,  $\tilde{C}^{(2)}$  and  $\tilde{C}^{(3)}$ , which describe deformation of each sublaminates, can be proved to be equal since the displacements of each sublaminates are the same at the interface between the adjacent sublaminates. In addition, it is clear that the force and the moments reacted on the whole of the laminate are equal to the sums of the corresponding force and moments on each sublaminates. Hence we obtain the following reduced constitutive equations for the whole of the laminate.

$$\tilde{N}^{LAM} = \tilde{H}^{LAM} \tilde{C}^{LAM} \quad (19)$$

Where,

$$\begin{aligned} \tilde{N}^{LAM} &= \tilde{N}^{(1)} + \tilde{N}^{(2)} + \tilde{N}^{(3)} \\ \tilde{H}^{LAM} &= \tilde{H}^{(1)} + \tilde{H}^{(2)} + \tilde{H}^{(3)} \\ \tilde{C}^{LAM} &= \tilde{C}^{(1)} = \tilde{C}^{(2)} = \tilde{C}^{(3)} \end{aligned} \quad (20)$$

Superscript  $LAM$  denotes the whole of the laminate. We get deformation of each sublaminates by solving the constitutive Equation 19. By substituting  $\tilde{C}^{(1)}$ ,  $\tilde{C}^{(2)}$

and  $\tilde{C}^{(3)}$  to Equation 17 and using Equation 16, we can obtain strains and curvature,  $\varepsilon_y^{(0(\lambda))}$ ,  $\gamma_{xy}^{(0(\lambda))}$  and  $\kappa_y^{(\lambda)}$  of each sublaminates from Equation 14 written in terms of the  $\lambda$ -th sublaminates.

#### 2.4. Simplified method for determining mode components of strain energy release rate of a free-edge delamination

We can get the strain-energy release per unit length of the laminate caused by the onset of a delamination crack of length  $a$  as follows,

$$U(a) = \frac{1}{2} (N_x^{LAM} \varepsilon_0^{LAM} + M_x^{LAM} \kappa_x^{LAM} + M_{xy}^{LAM} \kappa_{xy}^{LAM} + T_x^{LAM} \omega_x^{LAM}) \quad (21)$$

We obtain the following equation for the total strain energy release rate under the constant displacement condition.

$$G(a) = -\frac{U(a + \Delta a) - U(a)}{\Delta a} \quad (22)$$

Where,  $\Delta a$  is a virtual crack propagation length.

As mentioned in Section 2.1, a peeling stress occurs at the interface  $z = z_i$  in the free-edge boundary when the interface moment,  $m(z_i)$ , is positive. If a delamination crack of length  $a$  with the opening mode (Mode I) is generated, we can calculate the opening angle of the crack by  $[\kappa_y^{(3)} - \kappa_y^{(2)}]a$ , where  $\kappa_y^{(3)}$  and  $\kappa_y^{(2)}$  represent the curvature of sublaminates above and below the interface  $z = z_i$  along which delamination occurs, respectively. We get the Mode-I strain energy release by the onset of the delamination crack as follows,

$$U_I(a) = \frac{1}{2} m(z_i) [-\kappa_y^{(3)} + \kappa_y^{(2)}] a \quad (23)$$

We can obtain the inplane sliding displacement of the crack by  $[\varepsilon_y^{(0(3))} - \varepsilon_y^{(0(2))}]a$ , and the anti-plane tearing displacement of the crack by  $[\gamma_{xy}^{(0(3))} - \gamma_{xy}^{(0(2))}]a$  as well. Using the interface shear forces  $q_y(z_i)$  and,  $q_x(z_i)$  we get Mode-II and Mode-III strain energy release due to the onset of the delamination crack by the following equations, respectively.

$$U_{II}(a) = \frac{1}{2} q_y(z_i) [\varepsilon_y^{(0(3))} - \varepsilon_y^{(0(2))}] a \quad (24)$$

$$U_{III}(a) = \frac{1}{2} q_x(z_i) [\gamma_{xy}^{(0(3))} - \gamma_{xy}^{(0(2))}] a$$

We can, therefore, calculate the Mode-I, Mode-II and Mode-III component of SERR for the free-edge delamination of length  $a$  by the following equations, respectively.

$$\begin{aligned} G_I(a) &= U_I(a)/a = \frac{1}{2} m(z_i) [-\kappa_y^{(3)} + \kappa_y^{(2)}] \\ G_{II}(a) &= U_{II}(a)/a = \frac{1}{2} q_y(z_i) [\varepsilon_y^{(0(3))} - \varepsilon_y^{(0(2))}] \\ G_{III}(a) &= U_{III}(a)/a = \frac{1}{2} q_x(z_i) [\gamma_{xy}^{(0(3))} - \gamma_{xy}^{(0(2))}] \end{aligned} \quad (25)$$

TABLE I Material properties and geometry of the laminate

$E_L = 138.6$ GPa	$E_T = 10.07$ GPa
$G_{LT} = 4.117$ GPa	$G_{LT} = 3.873$ GPa
$\nu_{LT} = 0.320$	$\nu_{TT} = 0.300$
$b$ (Semi-width) = 15 mm	
$h$ (Laminate thickness) = $6h_0 = 0.84$ mm	
$h_0$ (Ply thickness) = 0.14 mm	

$L$  denotes the fiber direction and  $T$  denotes the transverse direction

### 3. Numerical examples and discussion

The proposed method is applied to determine the mode components of SERR for free-edge delaminations in a  $[30/-30/90]_s$  composite laminate under uniform axial extension. The material properties and the geometry of the laminate are given in Table I. Free-edge delaminations exist at the interfaces which are symmetrically located with respect to the  $z = 0$  plane (mid-plane) and the  $y = 0$  plane as shown in Fig. 1. Because of symmetries, only one quarter of the  $x = 0$  section was analyzed. We used a generalized quasi-three dimensional finite element method [8] with the virtual crack closure technique to evaluate the accuracy of the present simplified method. The FEM code uses eight-node quadrilateral isoparametric elements.

Most analyses to obtain the SERR for composite laminates with delamination assume that individual plies or ply groups may be modeled as homogeneous and orthotropic. When this assumption is adopted and the delamination is between plies at dissimilar angles, a linear elastic analysis will predict a near-field oscillatory singularity to exist and the individual SERR components cannot be uniquely defined [10]. Raju, Crews and Aminpour [10] analyzed the individual SERR components by the finite element model with a thin resin layer at the delamination interface to eliminate the oscillatory singularity. They showed that the finite element model with the ‘bare’ interface, where the resin layer does not exist, is a very good approximation to the case with the interface resin layer, when the virtual crack propagation length  $\Delta a$  is either 0.25 or 0.5 of the ply thickness  $h_0$ . Hence we took  $\Delta a/h_0 = 0.36$  in FEM. We analyzed three cases, that is (1)  $[30/-30/90]_s$  laminate with delaminations at the 30/–30 interfaces, (2)  $[30/-30/90]_s$  laminate with asymmetric delaminations at the 30/90 interface, and (3)  $[-40/50_2/-40/40/-50_2/40]$  antisymmetry laminate with delaminations at –40/40 interface.

#### 3.1. $[30/-30/90]_s$ laminate with delaminations at the 30/–30 interfaces

Fig. 7 shows the individual components of SERR for  $[30/-30/90]_s$  laminate with delaminations at the 30/–30 interfaces. The Mode-I, Mode-II and Mode-III components of SERR calculated by Equation 25 are in well agreement with the FEM, when the delamination length is approximately more than the laminate thickness and when the delamination length is not too long. The mode components of SERR obtained from the FEM decrease as the delamination almost grows up across the laminate width. The total SERR calculated by Equation 22 coincides with the FEM when the delamination length is not too short or long.

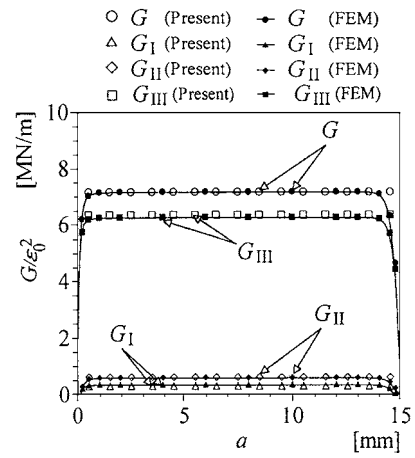


Figure 7 Strain energy release rate for  $[30/-30/90]_s$  laminate with free-edge delaminations at 30/–30 interfaces.

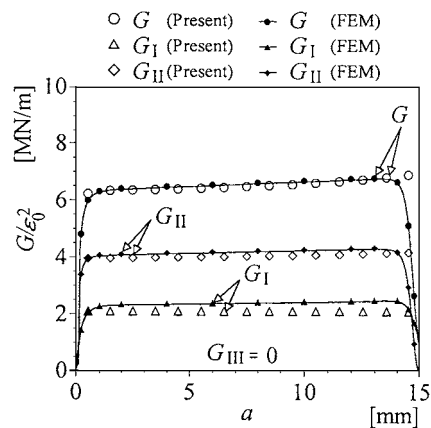


Figure 8 Strain energy release rates for  $[30/-30/90]_s$  laminate with free-edge delaminations at –30/90 interface.

#### 3.2. $[30/-30/90]_s$ laminate with asymmetric delaminations at the –30/90 interface

Fig. 8 shows the individual components of SEER for  $[30/-30/90]_s$  laminate with delaminations asymmetric located with respect to the laminate midplane at the –30/90 interface.

The Mode-I, Mode-II and Mode-III components of SERR calculated by Equation 25 are in well agreement with the FEM results, when the delamination length is not too long. The mode components of SERR obtained from the FEM decrease as the delamination increases across the laminate width. The total SERR calculated by Equation 22 coincides with the FEM when the delamination length is neither too short nor too long. For this case, however, the increase of the energy release rate is clearly recognized as the delamination grows. The results of the energy release rate analysis suggest that the behavior of the laminate depends on the position of the delamination interface.

#### 3.3. $[-40/50_2/-40/40/-50_2/40]$ anti-symmetry laminate with delamination at –40/40 interface

Li [11] analyzed the SERR for  $[-\theta/(90 - \theta)_2/-\theta/\theta/(\theta - 90)_2/\theta]$  anti-symmetry laminate with delamination

TABLE II The SERR at  $-40/40$  interface

[MN/m]	(a) Simplified method	FEM
$G_I/\varepsilon_0^2$	0.000	0.000
$G_{II}/\varepsilon_0^2$	0.000	0.000
$G_{III}/\varepsilon_0^2$	1.085	0.912
$G/\varepsilon_0^2$	0.910	0.912
[MN/m]	(b) By Li [11]	FEM
$G_I/\varepsilon_0^2$	0.032	-
$G_{II}/\varepsilon_0^2$	0.000	-
$G_{III}/\varepsilon_0^2$	0.083	-
$G/\varepsilon_0^2$	0.115	-

at each interfaces when  $\theta = 40^\circ$ ,  $[-40/50_2/-40/40/-50_2/40]$ . The results of SERR for  $[-40/50_2/-40/40/-50_2/40]$  with delamination at  $-40/40$  interface are shown in Table II. The SERR was analyzed by the present method and the FEM at the similar boundary conditions such as bending and twist to the existing analysis.

In case of the Li's analysis, there is no other numerical analysis except the simplified method. The results of the simplified method by Li shown in Table II (b) is about 1/10 of the results by the present method shown in Table II (a) or the FEM shown in Table II (a). Li is the one and only analyst who analyzed the SERR for anti-symmetry laminate.

The results of the presented method show approximately good agreement with that of the FEM.

### 3.4. Discussion

Wang [12] showed that the SERR increases to a maximum value with increasing delamination length, beyond which it remains constant. He called the delamination length at which this transition occurs as a characteristic delamination length. When predicting the onset and growth of free-edge delaminations, it is becoming relatively accepted to determine the SERR for a delamination of the characteristic length or greater, and then to compare the calculated SERR to the critical value. The present method gives a good estimation the individual components of SERR for the delamination of the characteristic length or greater.

The present method does not need the near-field information such as the displacement field or the distribution of the interlaminar stresses. Hence this method is not concerned with the oscillatory singularity. And, the analysis provides closed-form expressions for the Mode-I, Mode-II and Mode-III component of SERR. The simple nature of the method makes it suitable for primary design analysis for the delaminations of composite laminates.

The results of the present method were compared with that of the existing method calculated by Li. Only Li analyzed the SERR for anti-symmetry laminate. The results of the simplified method by Li are about 1/10 of the results by the presented method or the FEM.

### 4. Conclusions

Based on the previous sections, the following conclusions can be drawn.

1. A simplified method for determining the mode components of the strain energy release rate (SERR) of free-edge delaminations in composite laminates was developed. The method is based on a generalized quasi-three dimensional analysis modified by the classical laminated plate theory. The analysis provides closed-form expressions for the Mode-I, Mode-II and Mode-III components of SERR.

2. The individual mode components of SERR obtained by the presented method are in good agreement with a finite element analysis using the virtual crack closure technique.

It is shown that the presented method can be applied to any cases of the composite laminates such as the symmetric laminates with symmetric and asymmetric delaminations at each interfaces and the anti-symmetric laminates with delaminations at each interfaces.

### References

1. R. B. PIPES and N. J. PAGANO, *J. of Composite Materials* **4** (1970) 538.
2. E. F. RYBICKI, D. W. SCHMUESER and J. FOX, *ibid.* **11** (1977) 470.
3. A. S. D. WANG and F. W. CROSSMAN, *J. of Composite Materials Supplement* **14** (1980) 71.
4. T. K. O'BRIEN, "Characterization of Delamination Onset and Growth in a Composite Laminate" (Damage in Composite Materials, ASTM STP 775, 1982) p. 140.
5. T. AOKI and K. KONDO, *J. of the Japan Society for Composite Materials* **15** (1989) 166.
6. E. A. ARMANIOS and L. W. REHFELD, *J. of Composites Technology & Research* **11** (1989) 135.
7. R. A. SCHAPERLY and B. D. DAVIDSON, *Applied Mechanics Reviews* **43**(5), Part 2 (1990) S281.
8. K. KUNOO, N. UDA, K. ONO and K. ONOHARA, *Theoretical and Applied Mechanics* **41** (1992) 137.
9. J. C. HALPIN, in "Primer on Composite Materials: Analysis" (Technomic Publishing Co., 1984) p. 90.
10. I. S. RAJU, J. H. CREWS and M. A. AMINPOUR, *Engineering Fracture Mechanics* **30** (1988) 383.
11. J. LI, in "The 33rd AIAA etc., Structures, Structural Dynamics and Materials Conference, Part 1, 1992" (1992) p. 525.
12. S. S. WANG, *AIAA Journal* **22** (1984) p. 256.

Received 2 February  
and accepted 11 December 2001